

Hole-doping effect on the thermoelectric properties and electronic structure of CoSiC. S. Lue,^{1,*} Y.-K. Kuo,^{2,†} C. L. Huang,¹ and W. J. Lai¹¹*Department of Physics, National Cheng Kung University, Tainan 70101, Taiwan*²*Department of Physics, National Dong Hwa University, Hualien 97401, Taiwan*

(Received 3 December 2003; published 23 March 2004)

We report the effect of Al substitution on the temperature-dependent electrical resistivity, Seebeck coefficient, as well as thermal conductivity in the binary compound cobalt monosilicide. It is found that the substitution of Al onto the Si sites causes a dramatic decrease in the electrical resistivity and lattice thermal conductivity. A theoretical analysis indicated that the reduction of lattice thermal conductivity arises mainly from point-defect scattering of the phonons. For $x \geq 0.05$ in the $\text{CoSi}_{1-x}\text{Al}_x$ system, the Seebeck coefficient changes sign from negative to positive, accompanied by the appearance of a broad maximum. These features are associated with the change in the electronic band structure, where the Fermi level shifts downwards from the center of the pseudogap due to hole-doping effect. While the thermoelectric performance improves with increasing Al substitution, the largest figure-of-merit ZT value among these alloys is still an order of magnitude lower than the conventional thermoelectric materials.

DOI: 10.1103/PhysRevB.69.125111

PACS number(s): 72.15.Eb, 72.15.Jf, 71.20.Be

I. INTRODUCTION

Transition-metal silicides with semiconducting or semimetallic properties have attracted considerable attention due to their practical applications in electronics and thermoelectrics.^{1,2} Cobalt monosilicide CoSi has been reported to be one of the promising candidates for advanced thermoelectric applications.^{3,4} Previous transport studies on this compound indicated that CoSi is a semimetal with the room-temperature electrical resistivity (ρ) on the order of $1 \text{ m}\Omega \text{ cm}$.^{5,6} The Seebeck coefficient S is negative, with a moderate absolute value of $\approx 80 \mu \text{ V/K}$ at 300 K .³ On the other hand, the thermal conductivity κ , a combination of lattice contribution (κ_L) and electronic contribution (κ_e), is as high as 20 W/mK at room temperature. The electronic term estimated from the Wiedemann-Franz law $\kappa_e = TL_o/\rho$ (where the Lorentz number $L_o = 2.45 \times 10^{-8} \text{ W}\Omega/\text{K}^2$) is only 0.7 W/mK at 300 K , suggesting that the lattice phonons are responsible for the observed large thermal conductivity.

In general, the efficiency of a thermoelectric material is given by the dimensionless figure-of-merit $ZT = S^2T/\rho\kappa$. The energy conversion efficiency of a thermoelectric material increases with increasing ZT value. However, the difficulty in achieving good thermoelectric performance is characterized by the need to minimize the thermal conductivity of materials, while enhancing their electrical conductivity. The strategy to optimize these two conflicting parameters usually involves the increase of charge carrier by doping and the enhancement of phonon scattering by introducing crystallographic disorder.⁷

In this study, we investigated the effects of chemical substitution on the thermoelectric properties including electrical resistivity, Seebeck coefficient, as well as thermal conductivity for $\text{CoSi}_{1-x}\text{Al}_x$ ($0 \leq x \leq 0.15$). A significant decrease of lattice thermal conductivity accompanied by a large enhancement of electrical conductivity was observed as partially substituting Al onto the Si sites in CoSi. An analysis of lattice thermal conductivity further indicated that the point-defect scattering of the phonons plays an important role for the

reduction of κ_L . In addition, the evolution of the Seebeck coefficient in this class of materials was used to characterize the electronic structure in the region of the semimetallic pseudogap, in accordance with the band-structure calculations.

II. EXPERIMENTAL DETAILS AND RESULTS**A. Sample preparation and structural analysis**

Polycrystalline $\text{CoSi}_{1-x}\text{Al}_x$ samples were prepared by mixing appropriate amounts of elemental metals. Mixture of high-purity elements was placed in a water-cooled copper crucible and then melted several times in an argon arc-melting furnace. An x-ray analysis taken with Cu $K\alpha$ radiation on powder specimens was consistent with the expected $B20$ -type structure,⁸ with no other phases present in the diffraction spectrum, as demonstrated in Fig. 1(a). The variation of lattice parameter as a function of Al concentration is shown in Fig. 1(b). It is clearly seen that the lattice parameter increases with x , indicating that the Si sites are successfully replaced by Al atoms, according to the Vegard's law. It should be addressed that two samples with $x = 0.20$ and 0.30 were also fabricated. Although their x-ray spectra show single phase, the relative intensity of the diffraction peaks indicates strong disorder occurring in both materials. In this regard, the solubility limit for Al in the CoSi lattice is about $x = 0.15$ using our growth method.

B. Electrical resistivity

Electrical resistivity for the $\text{CoSi}_{1-x}\text{Al}_x$ alloys was obtained by a standard dc four-terminal method during warming process. The evolution of electrical resistivity with Al substitution is presented in Fig. 2. For all studied samples, the electrical transport exhibits metallic behavior (positive temperature coefficient). Upon Al substitution for Si, the electrical resistivity of the $\text{CoSi}_{1-x}\text{Al}_x$ alloys shows a significant reduction with increasing x . Such a result is attributed to an increase of hole carriers via substitution, as Al has

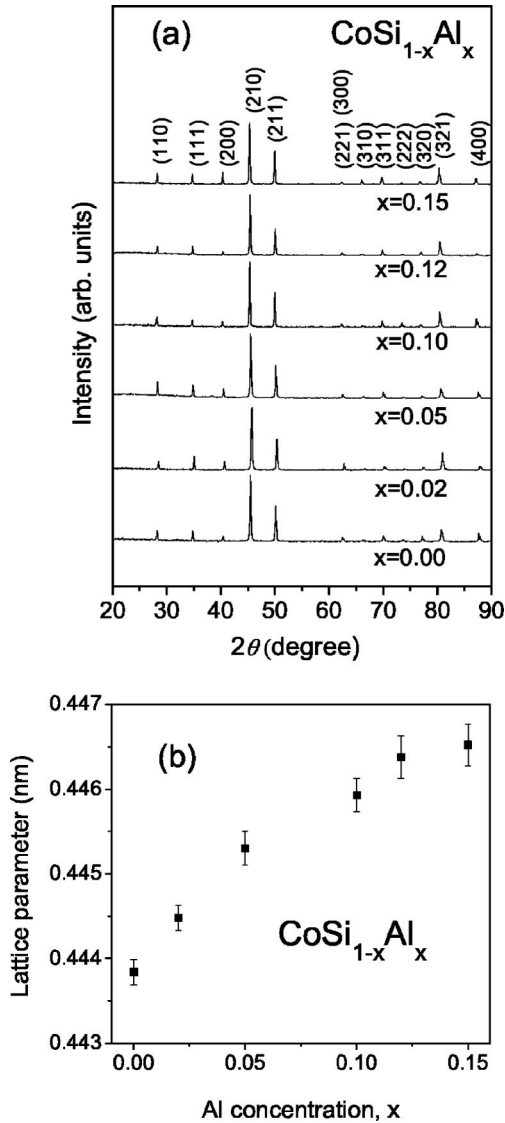


FIG. 1. (a) X-ray-diffraction patterns in $\text{CoSi}_{1-x}\text{Al}_x$. (b) Lattice parameter vs Al concentration as obtained from x-ray diffraction.

one more hole in its valence shell than Si. It is worthwhile mentioning that a 20-fold decrease in ρ is obtained with 15% Al substitution ($x=0.15$) than the CoSi sample.

C. Seebeck coefficient

Seebeck coefficients for the $\text{CoSi}_{1-x}\text{Al}_x$ series were measured with a dc pulse technique. Seebeck voltages were detected using a pair of thin Cu wires electrically connected to the sample with silver paint at the same positions as the junction of differential thermocouple. The stray thermal emfs are eliminated by applying long current pulses (~ 100 s) to a chip resistor which serves as a heater, where the pulses appear in an off-on-off sequence.

The T -dependent Seebeck coefficient of $\text{CoSi}_{1-x}\text{Al}_x$ is shown in Fig. 3. The negative S values for the stoichiometric compound of CoSi indicate that electron-type carriers dominate the heat transport in the entire temperature range we investigated, consistent with the previous results.³⁻⁵ For the

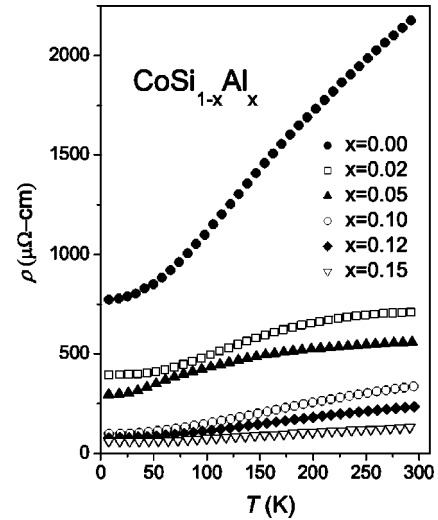


FIG. 2. Electrical resistivity as a function of temperature for $\text{CoSi}_{1-x}\text{Al}_x$.

slightly substituted sample ($x=0.02$), the S values remain negative regardless of a positive peak at low temperatures. Note that the absolute value of S for $\text{CoSi}_{0.98}\text{Al}_{0.02}$ is considerably smaller than that of CoSi . Such a result can be ascribed to the compensation of p - and n -type carriers involved in the heat transport processes by substitution. Upon further Al substitution for Si ($x \geq 0.05$), the hole concentration increases and consequently reverses the sign of S from negative to positive. In these alloys, the Seebeck coefficient develops broad maximums and the corresponding peak positions shift to higher temperatures with increasing x . The downturn in S at high temperatures is presumably due to the contribution of thermally excited quasiparticles across their pseudogaps. The observed Seebeck coefficients can be un-

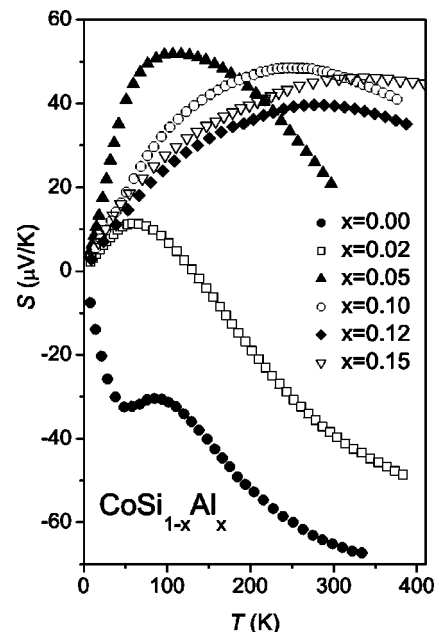


FIG. 3. Seebeck coefficient vs temperature in $\text{CoSi}_{1-x}\text{Al}_x$.

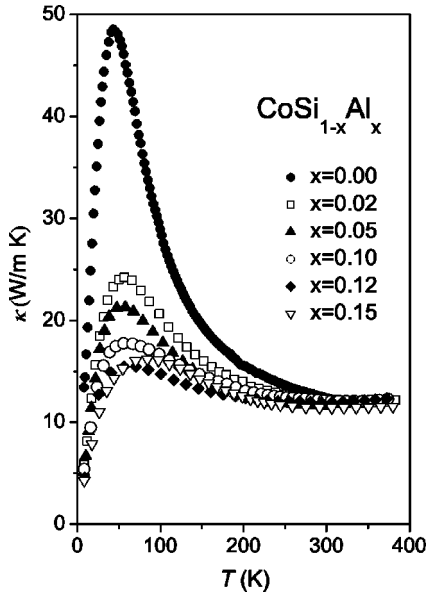


FIG. 4. Temperature dependence of the total thermal conductivity in $\text{CoSi}_{1-x}\text{Al}_x$.

derstood within the framework of two-carrier electrical conduction. Accordingly, the total S can be expressed as⁹

$$S = \left(\frac{\sigma_p S_p + \sigma_n S_n}{\sigma_p + \sigma_n} \right), \quad (1)$$

where $S_{p,n}$ and $\sigma_{p,n}$ represent the Seebeck coefficients and electrical conductivities for the p - and n -type carriers, respectively. Since the signs of S_p and S_n are opposite, tuning these quantities could result in a sign change in S , as we did observe in the present study.

D. Thermal conductivity

To further evaluate the possibility for potential thermoelectric applications in these materials, we performed T -dependent thermal-conductivity measurements. Thermal-conductivity measurements were carried out in a closed-cycle refrigerator, using a direct heat-pulse technique. Samples were cut to a rectangular parallelepiped shape of typical size of $1.5 \times 1.5 \times 5.0 \text{ mm}^3$ with one end glued (with thermal epoxy) to a copper block that served as a heat sink, while a calibrated chip resistor as a heat source glued to the other end. The temperature difference was measured by using an E -type differential thermocouple with junctions thermally attached to two well-separated positions along the sample. The temperature difference was controlled to be less than 1 K to minimize the heat loss through radiation, and the sample space is maintained in a good vacuum ($\approx 10^{-4}$ torr) during measurements. All experiments were performed on warming with a rate slower than 20 K/h. The uncertainty of our thermal conductivity is about 20%, mainly arising from the error on the determination of the geometrical factor of these samples.

In Fig. 4, we display the observed thermal conductivity for all studied samples. At low temperatures, κ increases with temperature and a maximum appears between 40 K and

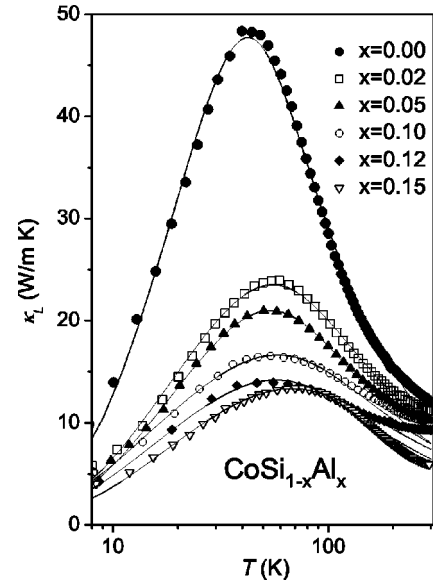


FIG. 5. Lattice thermal conductivity for $\text{CoSi}_{1-x}\text{Al}_x$ vs temperature. The solid lines represent the calculation based on Eqs. (2) and (3).

70 K. This is a typical feature for the reduction of thermal scattering in metals at low temperatures. A remarkable trend found in κ is that the height of the low-temperature peak decreases dramatically with increasing substitution level, indicative of a strong enhancement in the phonon scattering by Al substitution. Generally, the total thermal conductivity for ordinary metals and semimetals is a sum of electronic and lattice terms. The electronic thermal conductivity κ_e can be evaluated using the Wiedemann-Franz law $\kappa_e \rho / T = L_o$ with the measured resistivity data. The lattice thermal conductivity κ_L , plotted in Fig. 5, is obtained by subtracting κ_e from the observed κ . As seen from Fig. 5, the values of κ_L reduce drastically with increasing x in $\text{CoSi}_{1-x}\text{Al}_x$. It is found that the peak value of κ_L decreases from 49 W/m K for CoSi to 13 W/m K for $\text{CoSi}_{0.85}\text{Al}_{0.15}$. This observation is quite surprising, with which 15 at. % of Al substitution of the Si site could lead to such a huge reduction in κ_L . An analysis regarding this issue will be described in the following section.

III. DISCUSSION

It is known that the Seebeck coefficient measurement is a sensitive tool of probing the energy relative to the Fermi surface and the results could reveal information about the Fermi-level band structure. From the band calculations, CoSi, characterized as a semimetal, has a slightly indirect overlap between electron and hole pockets, which yields a small density of states (DOS) at the Fermi surface.¹⁰ Although the hole pockets are heavier ($m_h \approx 6m_o$ and $m_e \approx 2m_o$),⁵ the electron pockets are larger than the hole ones, still leading to the n -type carriers dominate its transport properties. The observed negative Seebeck coefficient in CoSi is thus consistent with this two-carrier electrical conduction picture.

With replacing Si by Al, the ρ values decrease accompa-

nied by the sign change in S . These observations are associated with an increase of the number of hole carriers via Al substitution, as expected from the nominal valences of Si and Al. Since the DOS in the pseudogap is very small, a change in the carrier concentration would lead to an appreciable downward shift of the Fermi energy E_F within a simple rigid-band scenario. This shift reduces the electron pockets but enlarges the hole pockets, making the p -type carriers dominate the transport behavior. As the temperature increases further, intrinsic electrons and holes are excited across the pseudogap. If the electrons have a slightly higher mobility than the holes in these materials, the thermal transport is increasingly governed by n -type carriers and the positive Seebeck coefficient would decrease after passing through a broad peak, as we observed in these materials. In addition, with increasing x value E_F shifts from near the valley to slightly below the center of pseudogap, resulting in a higher activated energy for quasiparticles to be thermally excited across the pseudogap. Therefore, the S maximum shifting toward higher temperature with larger x can be qualitatively understood in terms of this picture.

Now we discuss the influence of Al substitution on the phonon scattering processes in these alloys. In order to clarify the origin of the significant reduction of κ_L , we modeled the T -dependent κ_L using the Debye approximation. Such an analysis has been successfully applied to the p -type skutterudites and other materials,^{11,12} and the obtained fitting parameters would provide information about the phonon scattering mechanisms in the studied samples. In the model of Debye approximation, κ_L is written as^{13,14}

$$\kappa_L = \frac{k_B}{2\pi^2 v} \left(\frac{k_B T}{\hbar} \right)^3 \int_0^{\theta_D/T} \frac{x^4 e^x}{\tau_p^{-1}(e^x - 1)^2} dx, \quad (2)$$

where $x = \hbar\omega/k_B T$ is dimensionless, ω is the phonon frequency, \hbar is the reduced Planck constant, k_B is the Boltzmann constant, θ_D is the Debye temperature, v is the average phonon velocity, and τ_p^{-1} is the phonon scattering relaxation rate. Here τ_p^{-1} is the combination of three scattering mechanisms and can be expressed as

$$\tau_p^{-1} = \frac{v}{L} + A\omega^4 + B\omega^2 T e^{-\theta_D/3T}, \quad (3)$$

where the grain size L and the coefficients A and B are the fitting parameters. The terms in Eq. (3) are the scattering rates for the grain-boundary, point-defect, and phonon-phonon Umklapp scatterings, respectively. In general, the grain-boundary scattering is a dominant mechanism for the low-temperature κ_L , while the Umklapp procedure is important at high temperatures. The point-defect scattering, on the other hand, has a strong influence on the appearance of the shape and position of the phonon peak occurring in the intermediate temperature regime. Taking $v = 5400$ m/s and $\theta_D = 410$ K given from the specific heat measurement for CoSi,¹⁵ the experimental data of all studied samples can be fitted very well for $T < 120$ K. The fitting curves are drawn as solid lines in Fig. 5, and the resulting parameters are listed in Table I. Notice that the fitting curves deviate from

TABLE I. Lattice thermal-conductivity fitting parameters determined from Eqs. (2) and (3).

x	L (μm)	A (10^{-42} s^3)	B (10^{-18} s/K)
0.00	9.44	0.60	4.54
0.02	5.81	1.67	2.94
0.05	5.14	1.84	3.62
0.10	7.68	3.34	2.37
0.12	5.82	3.66	3.21
0.15	4.74	4.01	2.45

the data points for $T > 120$ K. We attempted to include electron-phonon interaction in the calculations, but such an effort yielded no significant improvement to the overall fit. We thus conclude that electron-phonon scattering has a minor influence on the lattice thermal conductivity in $\text{CoSi}_{1-x}\text{Al}_x$. The discrepancy between the measured data and the fit at high temperatures may arise from radiation losses during the experiments, temperature dependence of the Lorentz number, and the undetermined Debye temperatures for the substituted compounds. This discrepancy, however, has little effect on the following discussion.

As seen from Table I, the grain size L for the studied materials varies from 5 to 9 μm with no obvious tendency among these samples. Also the Umklapp coefficient B scatters around in these samples, presumably due to the unknown Debye temperature for these materials (except CoSi). It should be noted that even though the Debye temperature is a significant factor for the Umklapp scattering rate, it only affects the fitting result at high temperatures. On the other hand, a systematic change of the parameter A is obtained from the fit, where A increases with increasing Al content. According to the model proposed by Klemens,¹⁶ the prefactor A is proportional to $c(1-c)$, where c is the relative concentration of point defects. As shown in Fig. 6, the parameter A scales linearly with $x(1-x)$, suggesting that the effect of Al substitution for Si in the $\text{CoSi}_{1-x}\text{Al}_x$ system is strongly related to the appearance of point defect. We argue that these

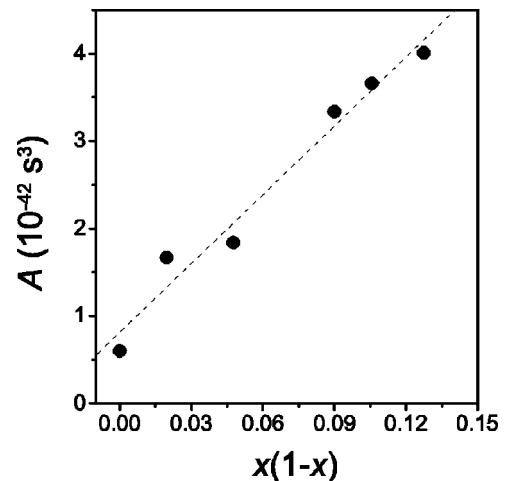


FIG. 6. Prefactor A as a function of $x(1-x)$ for $\text{CoSi}_{1-x}\text{Al}_x$.

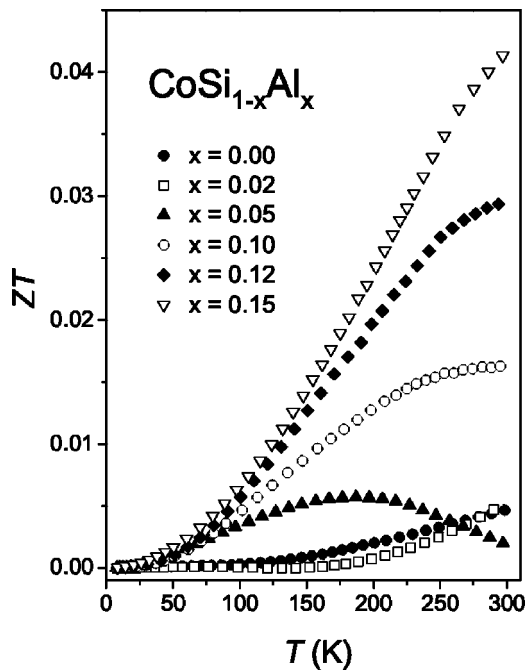


FIG. 7. ZT value as a function of temperature for $\text{CoSi}_{1-x}\text{Al}_x$.

point defects are not originated from the mass fluctuations between Si and Al, since their atomic size and mass differences are less than 4%. Rather, other lattice imperfections, such as vacancies, are introduced with Al substitution, which in turn give rise to a considerable amount of point defect to the substituted samples.

From the application viewpoint, the efficiency of a thermoelectric material is characterized by the dimensionless ZT value. For the present studied system, the ZT value increases significantly with increasing Al concentration, as demonstrated in Fig. 7. This is mainly due to the fact that both ρ and κ_L decrease drastically with Al substitution, although no

significant enhancement on the Seebeck coefficient is observed. As one can see from Fig. 7, an encouraging ten-time enhancement on the room-temperature ZT value between CoSi (0.0047) and $\text{CoSi}_{0.85}\text{Al}_{0.15}$ (0.041) is achieved. However, the highest ZT found among the studied compositions is still an order of magnitude smaller than that of the state-of-the-art thermoelectric materials such as Bi_2Te_3 .¹⁷

IV. CONCLUSIONS

A systematic study of the thermoelectric properties on $\text{CoSi}_{1-x}\text{Al}_x$ ($x=0.00-0.15$) was performed. Upon Al substitution for Si, the $\text{CoSi}_{1-x}\text{Al}_x$ alloys exhibit a significant reduction in ρ and a sign change in S , due to hole doping to the substituted samples. Besides, broad maximums in S are observed and the corresponding peak positions shift to higher temperatures for larger x . Such observations were attributed to the contribution of thermally excited quasiparticles across their pseudogaps and the latter feature was connected to the shift of Fermi energy E_F within the rigid-band scenario. Furthermore, the effect of Al substitution is strongly related to the appearance of point defects, which causes a drastic reduction of the lattice thermal conductivity. In this work we clearly demonstrate that Al substitution for the Si sites in CoSi represents a good opportunity for improving its ZT value, although these values are still small compared to the conventional thermoelectrics. Based on what we found in this investigation, an important issue which should be considered in future studies is the effect of n -type doping on the thermoelectric performance of the CoSi system.

ACKNOWLEDGMENTS

We thank Professor S. T. Lin of National Cheng Kung University in Taiwan for the help with sample preparation. This work was supported by National Science Council, Taiwan, under Grants Nos. NSC-92-2112-M-006-012 (C.S.L.) and NSC-92-2112-M-259-011 (Y.K.K.).

*Electronic address: cslue@mail.ncku.edu.tw

†Electronic address: ykkuo@mail.ndhu.edu.tw

¹*Thermoelectric Materials and New Approaches*, edited by T.M. Tritt, M. Kanatzidis, H.B. Lyon, Jr., and G.D. Mahan, Mater. Res. Soc. Symp. Proc. 478 (Materials Research Society, Pittsburgh, 1997).

²H. Lange, Phys. Status Solidi B **201**, 3 (1997).

³S. Asanabe, D. Shinoda, and Y. Sasaki, Phys. Rev. **134**, A774 (1964).

⁴S.W. Kim, Y. Mishima, and D.C. Choi, Intermetallics **10**, 177 (2002).

⁵G.T. Alekseeva, V.K. Zaitsev, A. Petrov, V.I. Tarasov, and M.I. Fedorov, Sov. Phys. Solid State **23**, 1685 (1981).

⁶E.N. Nikitin, Sov. Phys. Solid State **2**, 588 (1960).

⁷F.J. DiSalvo, Science **285**, 703 (1999).

⁸W.B. Pearson, *A Handbook of Lattice Spacings and Structures of Materials and Alloys* (Pergamon, Oxford, 1967); *Structure Reports* (International Union of Crystallography, Utrecht, 1967).

⁹A.F. Ioffe, *Physics of Semiconductors* (Infosearch Limited, London, 1960).

¹⁰E.N. Nikitin, P.V. Tamarin, and V.I. Tarasov, Sov. Phys. Solid State **11**, 2002 (1970).

¹¹J. Yang, in *Chemistry, Physics and Materials Science of Thermoelectric Materials, Beyond Bismuth Telluride*, edited by M.G. Kanatzidis, S.D. Mahanti, and T.P. Hogan (Kluwer Academic, Dordrecht, 2003), p. 169.

¹²D.G. Onn, A. Witek, Y.Z. Qiu, T.R. Anthony, and W.F. Banholzer, Phys. Rev. Lett. **68**, 2806 (1992).

¹³J. Callaway, Phys. Rev. **113**, 1046 (1959).

¹⁴J. Callaway and H.C. von Baeyer, Phys. Rev. **120**, 1149 (1960).

¹⁵A. Lacerda, H. Zhang, P.C. Canfield, M.F. Hundley, Z. Fisk, J.D. Thompson, C.L. Seaman, M.B. Maple, and G. Aeppli, Physica B **186**, 1043 (1993).

¹⁶P.G. Klemens, Proc. Phys. Soc., London, Sect. A **68**, 1113 (1959).

¹⁷*CRC Handbook of Thermoelectrics*, edited by D.M. Rowe (CRC Press, Boca Raton, FL, 1995).